Visakhapatnam Chapter

Proceedings of Indian Geotechnical Conference 2020
December 17-19, 2020, Andhra University, Visakhapatnam

Solutions for Foundation Systems Subjected to Earthquake Conditions

Deepankar Choudhury[1], Shibayan Biswas[2], Milind Patil[3] and Sujatha Manoj[4]

[1] Institute Chair Professor, Department of Civil Engineering, Indian Institute of Technology Bombay, Powai, Mumbai 400076, India
dc@civil.iitb.ac.in
[2] PhD Research Scholar, Department of Civil Engineering, Indian Institute of Technology Bombay, Powai, Mumbai 400076, India
shibayanbsws@gmail.com
[3] Former PhD Research Scholar, IITB-Monash Research Academy, Powai, Mumbai 400076, India
milind16288@gmail.com
[4] PhD Research Scholar, Department of Civil Engineering, Indian Institute of Technology Bombay, Powai, Mumbai 400076, India. Also, Technical Director, Mott MacDonald Singapore Pte Ltd, Singapore 189721
sujathamanoj@hotmail.com

Abstract. Soil-structure interaction plays an important role in dynamic behavior of a foundation under combined static and seismic loadings. This paper describes a few case histories with field studies of deeply embedded bridge foundations to showcase the earthquake induced lateral effects using finite element framework. Rigorous dynamic approach with detailed numerical analysis for large diameter pile foundation and pseudo-static approach for rigid caisson foundation presented in this study demonstrated the functionality of foundation systems in seismic conditions. Efficacy of barrettes over piles as a cost-effective foundation solution in high-rise buildings has also been discussed by obtaining higher resistance under static condition. Finally, an analytical methodology considering three-dimensional passive wedge developed in front of the rigid caissons is presented for estimating the ultimate soil resistance under seismic condition. Closed-form expressions to determine seismic passive earth pressure coefficient and its distribution along caisson length for different embedment ratio has been explained here that can be adopted in practice to analyze foundation systems subjected to earthquake condition.

Keywords: soil-structure interaction, pile, caisson, barrette, earthquake.

1 Introduction

Embedded foundation beneath the superstructure are designed to provide stability against several load combinations, that include dead load, live load, wind load and such others coming from both operational and environmental point of view. Whereas,

for heavy and important structures in high seismic zones, in addition to above mentioned axial and transverse loads, earthquake load needs to be included in the analysis to find the most critical load combinations [1-3]. Several practice codes and previous literature illustrated that the seismically induced lateral load set up a major challenge to the foundation design engineers. Over the past decades, foundations of different characteristics, shapes, sizes have been used by practicing engineers to cater the applied load. Among deeply embedded foundations, pile foundation, barrette foundation and caisson foundation are frequently adopted for bridges and tall buildings under both static and seismic conditions. Soil-pile interaction plays an important role in dynamic behavior of a deep foundation under combined static and seismic loading where the deformation and bending moment in the piles resulting from earthquake induced lateral effects are mainly determined. Although dynamic analysis of large diameter pile foundations [4] and subsequently combined pile-raft foundations have gained huge attention among researchers in recent years, barrette foundations with different orientations and shapes are considered as a potential foundation solution in future for high-rise buildings in different parts of the world [5]. Barrettes, differ from circular cast-in-situ reinforced concrete piles in both their shape and method of construction, these are considered as an efficient approach in carrying vertical loads [6] and thus regarded as a cost-effective alternative to the large diameter bored piles in cases of heavy structures that need to be built in small footprint areas. Although the loading direction and orientation of barrettes affect the horizontal capacity [7] in large extent, the efficiency under seismicity is yet to be proven and demands rigorous research. On the contrary, caisson foundations which are mainly used as foundation system of bridges, deep-water wharves and overpasses and sometimes as single foundation element of transmission towers and heliostats, are considered as immune to seismic loading due to its massive structure and higher rigidity [8, 9]. However, this assumption has been found to impart a fallacious hope only after several bridges founded on caissons were reported to encounter damage in Kobe 1995 earthquake. Therefore the solutions for foundation systems under earthquake loading possess the requirement of extensive research where both the stability and serviceability criteria along with cost-effectiveness can be taken care off.

This paper presents a detailed discussion on three different types of deeply embedded foundation systems where effectiveness of each of the foundation systems under seismic loading have been demonstrated categorically. Initially a case study comprising of dynamic analysis of a site of the proposed Mumbai Trans Harbour Link (MTHL) focusing on soil-structure interaction analysis of bridge foundation has been showcased. In this section, the deformation and bending moment in the large diameter piles resulting from earthquake induced lateral effects are determined through numerical method. Following, the effectiveness of barrette foundations over cast-in-situ large diameter piles due to the better orientation to the direction of the high horizontal loads and moments to efficiently offer higher resistance, has been discussed by presenting a suitable comparative study. Later, a case study of a river crossing bridge supported by rigid caisson foundation has been studied by adopting pseudo-static approach in finite element framework. Finally, an analytical methodology for estimat-

ing the ultimate soil resistance acting on rigid caissons under seismic condition has been presented as an efficient solution for foundation systems.

2 Large Diameter Pile Foundation

Effects of earthquake on large diameter pile foundation has been discussed in detail in this section of the paper. A case study of pile-structure interaction analysis of bridge foundation of the proposed Mumbai Trans Harbour Link (MTHL) under seismic loading conditions through numerical method has been demonstrated. The Mumbai Trans Harbour Link (MTHL) of length 21.8km has been planned to improve connectivity between Island city and main land (Navi Mumbai). The proposed site of MTHL is located at seashore zone of Mumbai coastal region in the Indian state of Maharashtra. The site comes in seismic zone III according to the latest seismic zonation map of India, which is available in the earthquake design code of India [10]. Earthquake response analysis of the site has been carried out in transverse direction for the predicted earthquake ground motion. The detailed analysis includes numerical investigation of soil-structure-interaction of bridge foundation under seismic loading conditions.

2.1 Soil strata and local geological condition

A number of boreholes have been studied to identify the critical section of the bridge. Boreholes were executed up to the depth of 37m below seabed level. The chart datum is at 3.3m above seabed level. From the bore log data, it is observed that the top soil layer of around 16m is predominantly a silty clay soil with fines content of 90% to 100%. From 16.5m to 27m depth, sub strata consist of basalt of poor to extremely good quality. The soil stratigraphy is simplified into a horizontally layered system of varying thickness. The material properties of soil and rock are listed in Table 1. The modulus of elasticity (E) of clayey soil has been determined from the correlation between E and C_u that is obtained from vane shear test, (E = 200*(C_u), [11]). Under earthquake loading, the behavior of soil is primarily governed by dynamic properties of the soil. Therefore, dynamic properties of material such as, shear wave velocity (vs) is treated as primary input parameter [12, 13].

2.2 Soil-structure interaction analysis of pile foundation

A horizontal ground motion accelerogram have been adopted under MCE conditions. Amplitude of vertical components are considered as two third of that of horizontal component [14]. Table 2 shows the main characteristics of components of ground motion for MCE condition. Figure 1 shows the accelerogram compatible to the 5% damped MCE level of design spectrum.

Table 1. Material properties of soil and rock

Description	Depth (m)	RQD (%)	Υ_{sat} (kN/m^3)	Υ_{dry} (kN/m^3)	E (MPa)	Poisson's ratio (v)	G (MPa)	$v_{s,30}$ (m/s)	UCS, σ_{ci} (MPa)
Very soft to stiff silty Clay	0 - 17.5	-	19.5	14.5	1.43	0.49	-	242.49	-
Slightly fractured, Moderately strong Basalt	17.5 - 23	79	-	26.94	4286	0.31	1635.878	779.249	41.03
Moderately weathered fractured Basalt	23 - 27	46	-	27.99	5249	0.30	2018.846	849.278	54.08
Slightly fractured, Moderately strong Basalt	27 - 37	100	-	25.68	6256	0.26	2482.54	983.219	43.14

Table 2. Main characteristics of input ground motion

Earth-quake ID	Earth-quake	PGA (g)	Duration (s)	Bracketed duration (s)	Significant duration (s)	Predominant frequency (Hz)
EQ1	H-MCE-1	0.329	40.45	30.51	15.38	5.55

The section of the bridge foundation of the MTHL is modelled by using a finite element computer program, PLAXIS3Dv.2017.01 [15]. The geometrical information relevant to the foundation is shown in Figure 2. The foundation section consists of four piles, each having length of 36.5 m and diameter of 2.2 m. Piles are connected to 3.3 m thick pile cap and then top of it there are two pier shafts of 15.134 m length and pier heads of 3 m. Bridge deck is rested on pier head with the help of elastomeric bearings. Each pier is loaded with 2000 Ton (20000 kN) of superstructure load. The superstructure load is simplified into surface load of 935 kN/m2 and applied directly at top of the pier head. Mean sea level considered at 5.81 m above seabed.

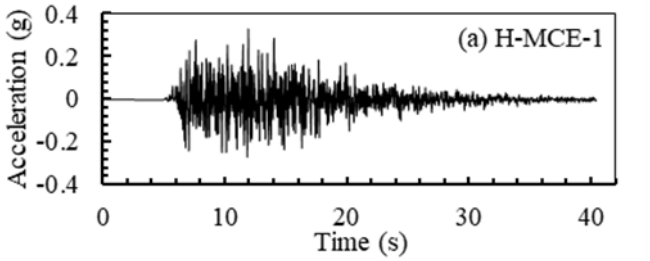

Fig. 1. Accelerogram (horizontal component) compatible to the 5% damped MCE

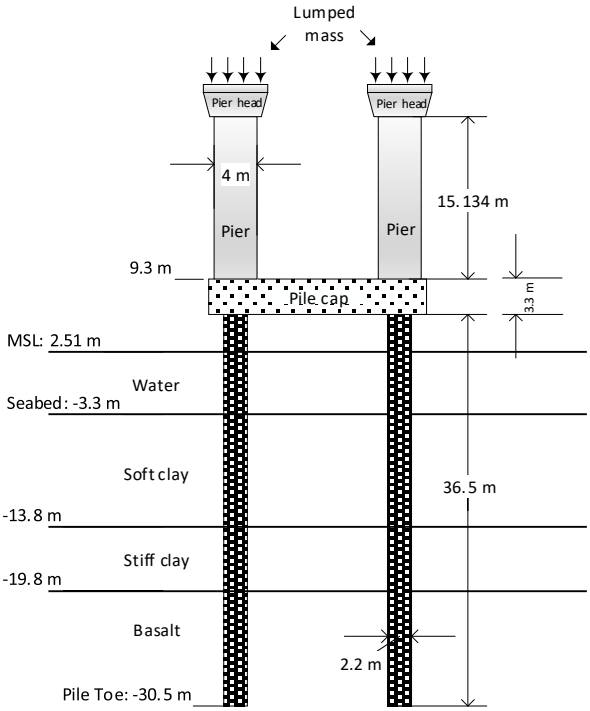

Fig. 2. Schematic illustration of geometrical and geological data relevant to the foundation

2.3 Numerical analysis

The soil model of dimensions 80 m x 40 m x 40.3 m has been adopted in the present analysis; the soil continuum is discretized with 10-noded tetrahedral elements. Soil materials are modelled using Mohr-Coulomb (MC) model [16], rock material modelled using Hoek-Brown criteria [17] and pile, pile cap, pier and pier cap are modelled using conventional Linear-Elastic (LE) constitutive behavior. The geotechnical properties of each layer adopted in the analysis are given in Table 3 and 4. Undrained shear strength of top 16.5 m soil is calculated by Equation 1.

$$S_u / p_o = 0.11 + 0.0037PI \quad (1)$$

Table 3. Input soil parameters considered in PLAXIS3D

Layer	Identification	Top (m)	Bottom (m)	Drainage type	γ_{unsat} (kN/m^3)	γ_{sat} (kN/m^3)	E (kN/m^2)	μ	c' (kN/m^2)	φ'(Degree)	Su (kN/m^2)
1	01-Soft silty clay	-3.3	-13.8	Undrained	13	14.2	9685	0.49	--	--	-33.26$^{\$}$
2	02-Stiff silty clay	-13.8	-19.8	Undrained	18	19.5	308966.4	0.49	--	--	-110.24$^{\$}$
3	03-Residual and weathered basalt	-19.8	-25.3	Undrained	22.48	23.5	1904056	0.35	500*	25*	--

*Hoek (2000) $^{\$}$Duncan and Buchignani (1976)

Table 4. Input soil parameters considered in PLAXIS3D

Layer	Identification	Top (m)	Bottom (m)	γ_{unsat} (kN/m^3)	E (kN/m^2)	μ	σ_{ci} (kN/m^2)	m_i[#]	GSI[#]	D[#]	ψ_{max}[#]
4	04-Slightly Fractured basalt	-25.3	-26.3	26.94	4294257.55	0.31	41030	17	35	0.8	7
5	05-Moderately weathered basalt	-26.3	-30.3	27.25	5118912.5	0.30	54080	17	45	0.7	10
6	06-Basalt I	-30.3	-32.3	27.57	3512418	0.30	50000[#]	17	55	0.6	21
7	07-Basalt II	-32.3	-33.3	25.78	5465195.01	0.28	46000[#]	17	51	0.6	14
8	08-Basalt III	-33.3	-35.3	25.68	6215094.14	0.26	43140	17	47	0.6	21
9	09-Basalt IV	-35.3	-37.3	27.67	4594776.44	0.25	38000[#]	17	43	0.6	16
10	10-Basalt V	-37.3	-40.3	24.68	4563332	0.25	33660	17	40	0.6	17

[#]Plaxis material manual

In static analysis, standard fixities were assigned to the model wherein the sides are restricted to move laterally, and the base is restrained in all directions. Whereas viscous boundaries are assigned to model under earthquake loading conditions. Four-pile configuration has been analyzed to investigate the effect of seismic loading on foundation system considering soil-structure interaction. Both piles and piers are modelled using volume element. Interface elements were added between pile and surrounding soil volume to allow for a proper modelling of soil-structure interaction. Average element size of soil continuum is 1.801m and virtual interface thickness factor used in

the analysis is 0.1 which results in to the interface thickness of 0.1801m. The roughness of the interaction was modelled by choosing a suitable value of the strength reduction factor (R_{inter}). In field, steel casing is to be provided for piles where it passes through the clayey soil. Therefore, R_{inter} of 0.6 and 0.75 was used for steel-soft clay interface and steel-stiff clay interface, respectively. Fully rigid interface behavior has been assumed between rock (basalt) and pile. The resistance offered by the top 16 m layer clay has been ignored in the seismic analysis of foundation system due to very soft characteristic of soil.

In non-linear fully dynamic numerical computation, the behavior of soil is primarily governed by dynamic properties of the soil. Therefore, dynamic soil properties are treated as primary input parameter along with strength parameter of the material. The simulation of the wave propagation problem through finite element (FE) analyses requires the appropriate definition of the input parameters for each sub-layer of the discretized deposit [18]. In fact, it is well-known that the solution strongly depends on the assumed profile of the stiffness and damping coefficients with depth. Under seismic loading conditions, soil is subjected to cyclic loading and unloading that generates hysteretic loop with the dissipation of energy and consequent damping. In constitutive modelling, inability of Mohr-coulomb model to simulate hysteretic damping was compensated using frequency-dependent Rayleigh formulation in terms of viscous damping [19]. Viscous boundary conditions are applied to vertical and base boundary. Input ground motion is applied at the base of the model in terms of prescribed displacement. Seismic analyses have been performed for predicted acceleration-time history (H-MCE-1).

2.4 Seismic response of sea-bridge foundation system

The performance of foundation system has been assessed under seismic conditions considering soil-structure interaction between soil and pile surface. Amplification of peak horizontal acceleration (PHA) from base surface to surface of soil model under predicted acceleration-time history has been plotted in Figure 3. The amplification of 1.41 for H-MCE-1 has been obtained from three-dimensional non-linear analysis using PLAXIS3Dv2017.01 [15]. Results of the analysis have been discussed further in detail. Figure 4 shows the three-dimensional view of the entire model and the pile, pile cap and piers that are modelled using volume element.

The vertical and lateral displacement contour diagrams under earthquake loading are plotted and are as shown in Figure 5. The highest values of shear strains observed in the upper layers of the soil deposit, where the minimum shear stiffness and the maximum damping ratio are attained as expected. There is negligible effect of earthquake on lateral displacement of piles and piers. This is attributed to 15m embedment of pile in basalt. The rock layers have contributed very less in amplifying the input ground motion. Figure 6 shows the shear stress and relative shear stress along the pile-soil interface surface due to combined loading. Structural forces in piles, axial force, bending moment and shear force under combined static and earthquake loadings are presented in Figures 7 and 8.

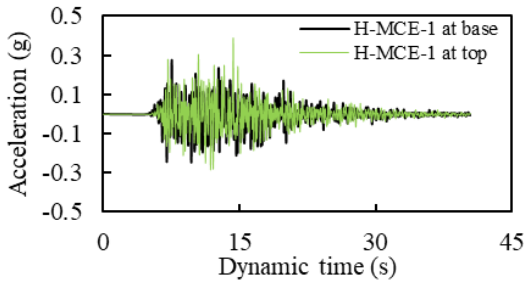

Fig. 3. Amplification obtained in PLAXIS3D in free-field condition under predicted accelerogram (horizontal component) of MCE level of design spectrum

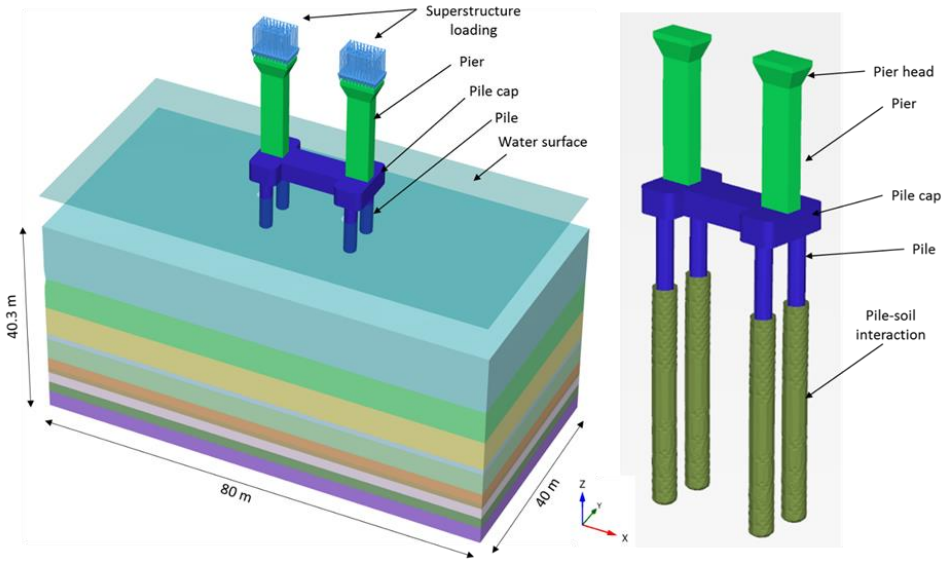

Fig. 4. Three-dimensional view of developed numerical model and highlighted view of piles, pile cap, piers, pier head, in PLAXIS3D

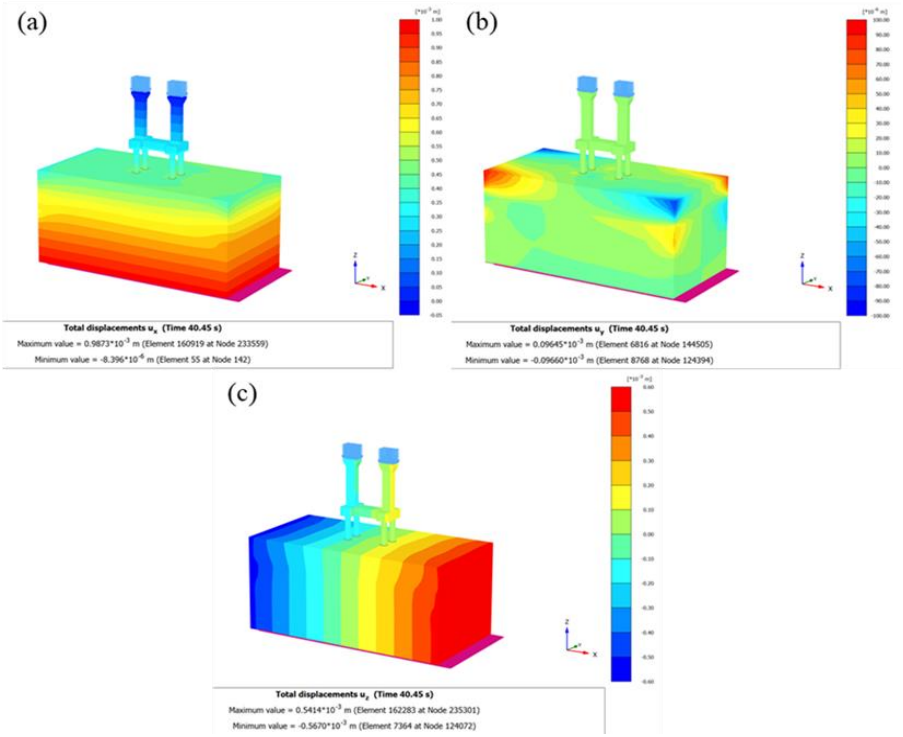

Fig. 5. Displacement due to earthquake loading in (a) x-direction, (b) y-direction, (c) z-direction

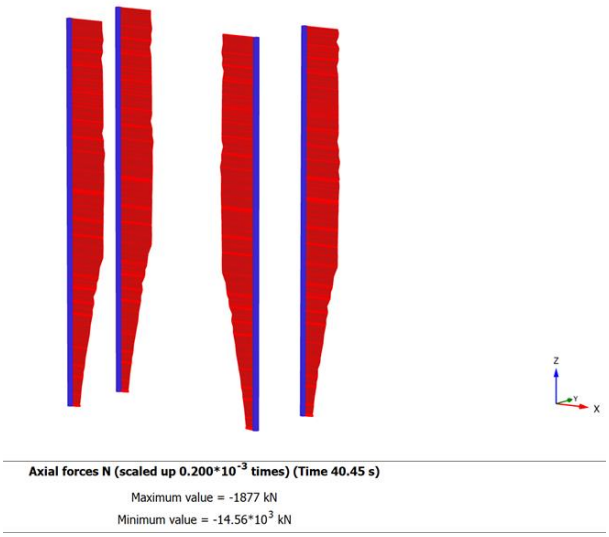

Fig. 6. Axial force in piles due to combined static and earthquake loadings

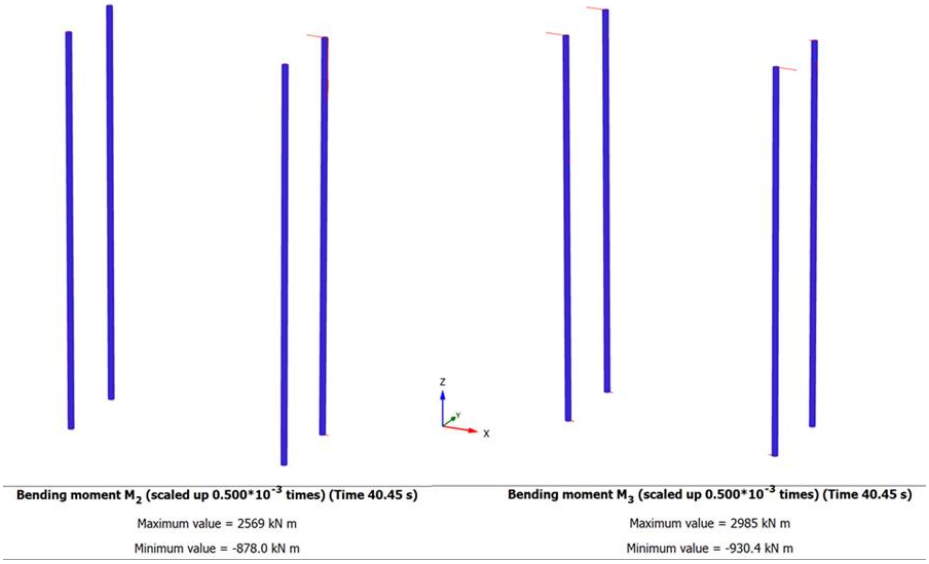

Fig. 7. Bending moment in piles due to combined static and earthquake loadings

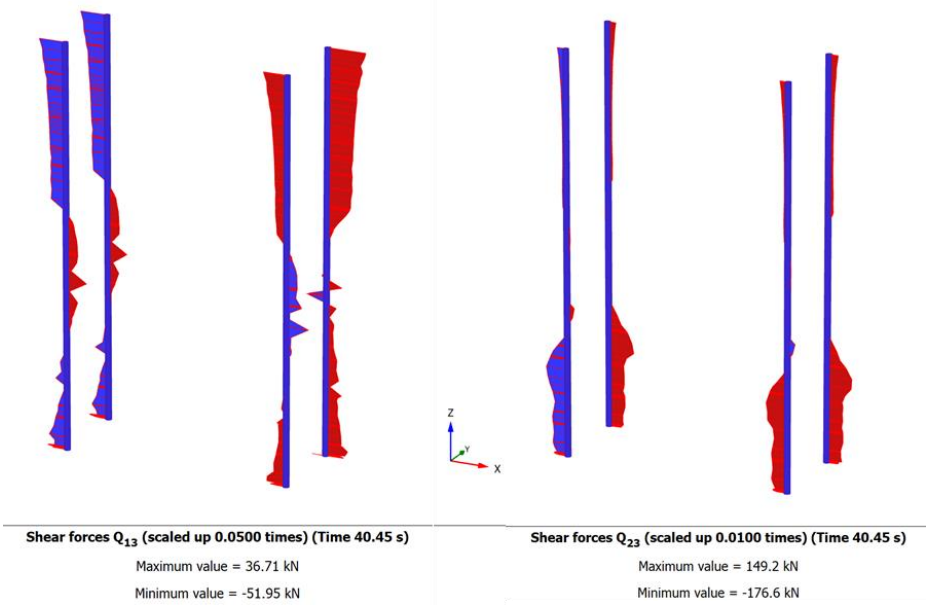

Fig. 8. Shear force in piles due to combined static and earthquake loadings

3 Barrette Foundations

Barrettes have several advantages over the typical circular pile of the same sectional area. Due to higher surface area compared to a bored pile of the equivalent section, there is more area available to develop skin friction which can result in significant increase of allowable bearing capacity depending on strata type and unit frictional resistance. Barrettes carry increased axial loads and moments and have higher shear capacities due to the increased specific surface area. The orientation and direction of loading affect the lateral resistance offered by barrettes. Barrettes can also have in general greater stiffness than bored piles. Thus, by orienting barrettes in load direction significantly higher lateral capacity than that by bored piles can be developed.

When large structures have to transfer heavy loads due to critical load combination due to earthquake and wind loads in addition to the dead load and wind loads, group interaction and group efficiency are critical [20-22]. Due to construction methodology used the barrettes verticality can be controlled effectively and higher capacity of barrettes decreases the number of elements in a group. Thus, the group efficiency increases significantly resulting in reduced construction time and cost.

3.1 Construction of Barrette Foundations

The construction method of barrettes is different from those of piles and the construction method chosen usually depends on the depth requirement, ground conditions and equipment availability. Barrettes are constructed using diaphragm wall cutters and grab-bucket or hydro fraise type drilling tools and the size of these tools used typically determines the size of foundation. They can be installed to large depths up to 100 m depth and depths in the range of up to 125m have been reported. The tool availability determines the size of barrettes of width in the range of 0.5, 0.6, 0.8, 1, 1.2 and 1.5 m and length in the range of 1.80, 2.20, 2.70 and 3.0m.

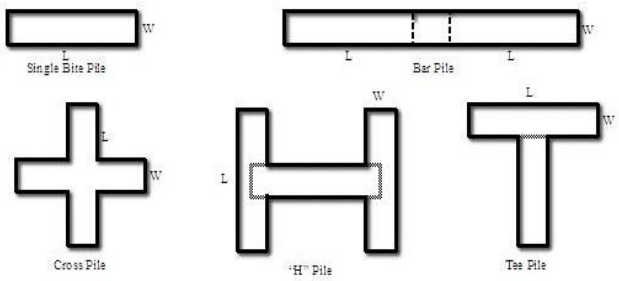

Fig. 9. Typical Shapes for Barrettes

In multiples of these dimensions, bigger or more rigid barrettes can be formed such as bars, crossed, H shaped or T shaped piles as shown in Figure 9. Barrettes are constructed mainly in three stages of operations namely, drilling, placing the reinforcement in place and concreting. The steps involved are as follows.

Construction of temporary guide walls and filling of the guiding trench with the thixotropic stabilizing fluid. Excavation through the supporting fluid suspension by means of a soil cutting grasp (clam shell grab) or hydro fraise, up to the required installation depth. In order to avoid instability of the trench, the level of the bentonite slurry in the excavation trench should at any moment be maintained at least 2 m above the highest water level in the full height trench, especially in the case of an artesian aquifer. De-sanding or replacement of the bentonite suspension, placement of the reinforcing cage and concreting with one of more tremie pipes, depending on the size of the barrette. As concreting progresses the concreting tube(s) is (are) pulled up gradually, during which the bottom is always be kept sufficiently deep in the already poured concrete, to avoid each interruption in the continuous concrete flow until the completion of the barrette.

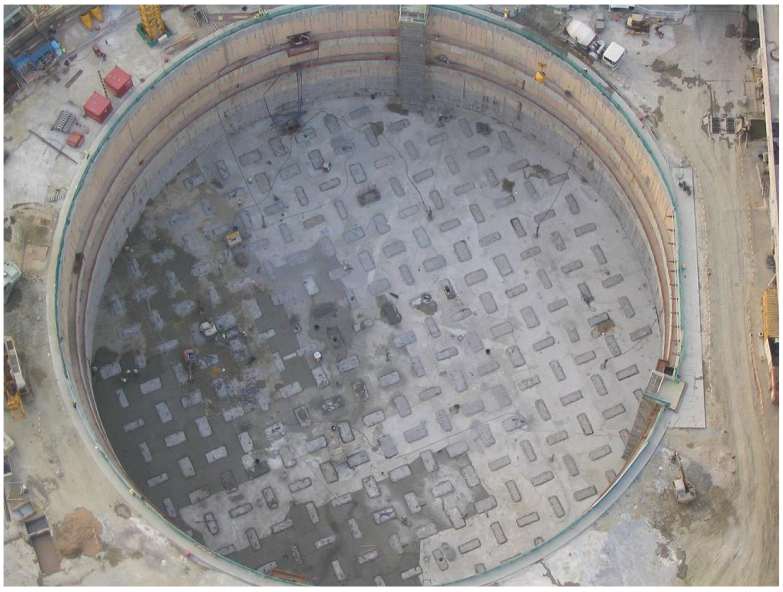

Fig. 10. Barrette foundation group of 290 barrettes China - Hong Kong, International Commerce Centre (PC Soletanche-Bachy, 2003)

They have the advantage over traditional rotary piles in that they can be installed to larger depths (over 100m deep) with great accuracy in verticality and can undertake much heavier working loads. One of the deepest Barrette foundations were constructed in Hongkong where they are installed about 125m below ground layout of which is shown in Figure 10.

3.2 Barrettes as efficient solution to cater to horizontal loads - Design example

As an alternative to the pile foundations Barrettes were selected to cater to heavy foundation loads of a 380m tall tower. Based on results of detailed geotechnical and

geophysical investigations a representative subsurface profile as shown in Figure 11. The design parameters presented in Table 5 are selected to design the tower foundations. Barrette capacities for the tower area was estimated considering cut-off level at -20.0m RL. Vertical and horizontal capacities of piles and barrettes are compared to evaluate the efficiency of foundation system for a tall tower as an example, in the below sections.

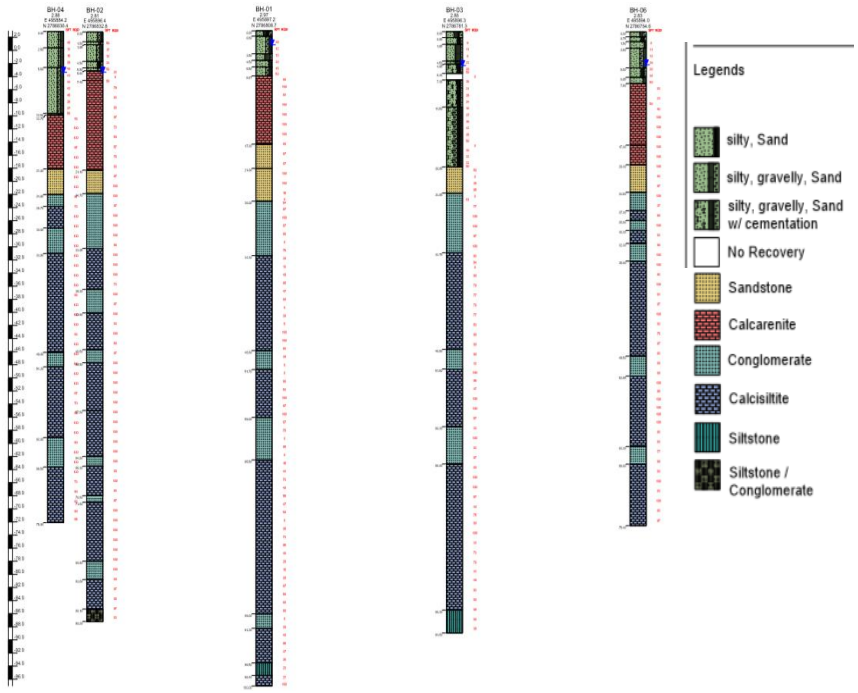

Fig. 11. Representative subsurface profile from design example site

3.3 Barrette and Piles - vertical capacities comparison

The maximum vertical loads for allowable stress design considering critical load combinations was of the order of 45 to 55MN for the tall tower considered in the example. The Barrette and Pile capacities for the same design profile are presented in Figure 12 below. From the graph, for a load of 54MN piles of 2000 mm diameters are required to be founded below -77m. The barrette size 1.2 x 2.8m (equivalent pile diameter of 2.07m) has 23% more perimeter. For a load of 50MN, barrettes of 1.2 x 2.8m size will have to extend to only -60m based on the capacity charts in Figure 12 whereas the 2000mm piles are required to go -71m which is 10m additional length.

Table 5. Design parameters from the example

Strata Description	Elevation (m) Top	Bottom	Thickness (m)	γ (kN/m^3)	UCS (Mpa)	φ' (°)	c' (MPa)	E (Mpa)	K_o
Calcarenite	-10.00	-14.20	4.20	20	2.20	39	0.20	185	0.371
Sandstone	-14.20	-23.00	8.80	20	0.75	41	0.07	110	0.344
Conglomerate 1	-23.00	-28.00	5.00	22	4.00	44	0.39	1100	0.305
Conglomerate 2	-28.00	-31.00	3.00	22	2.50	44	0.24	1100	0.305
Calcisiltite 1	-31.00	-47.00	16.00	20	1.17	37	0.08	150	0.398
Conglomerate 3	-47.00	-50.00	3.00	20	1.05	44	0.10	250	0.305
Calcisiltite 2	-50.00	-60.50	10.50	22	1.10	37	0.08	330	0.398
Conglomerate 4	-60.50	-63.80	3.30	20	1.15	43	0.11	700	0.318
Calcisiltite 3	-63.80	-90.00	26.20	22	1.30	37	0.08	350	0.398
Calcisiltite 4	-90.00	-100.0	10.00	20	1.50	37	0.10	200	0.398

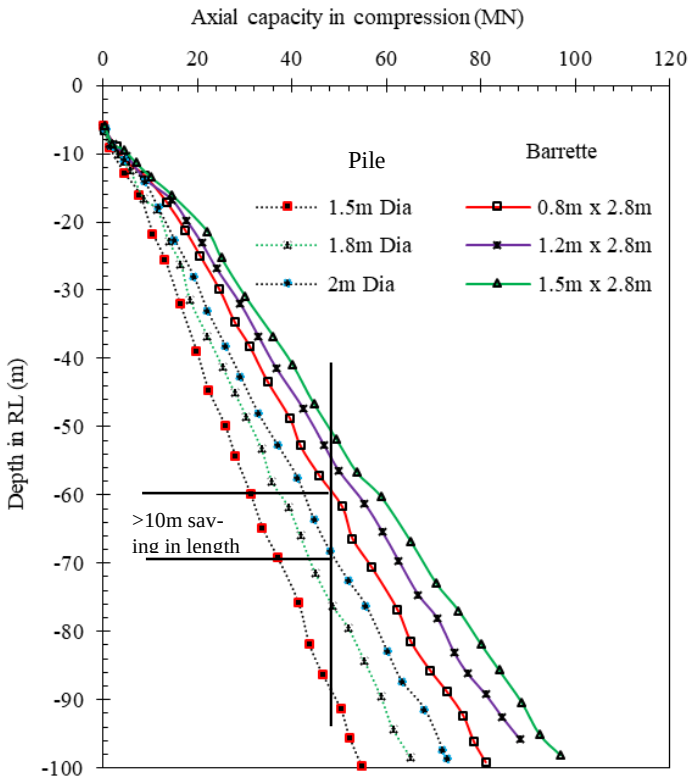

Fig. 12. Comparison of axial capacity values along depth of a 1.2 x 2.8 size barrette and equivalent 2m pile

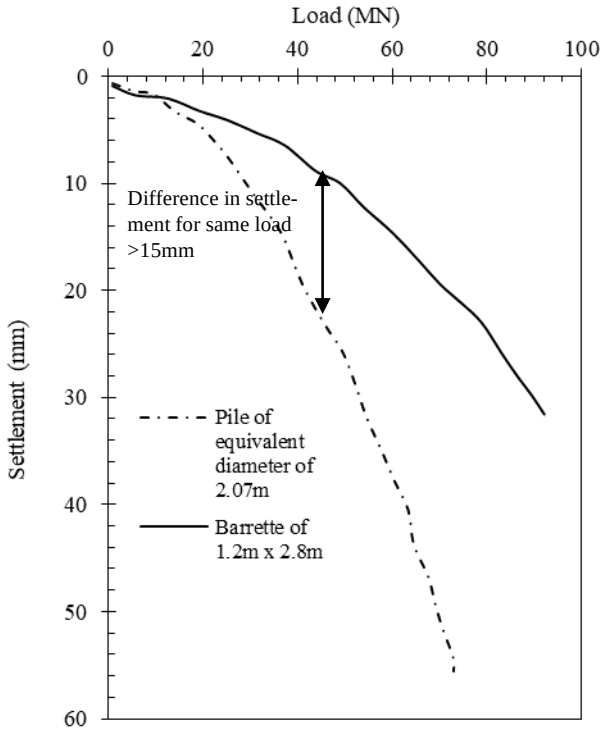

Fig. 13. Comparison of 1.2m x 2.8m size barrette and equivalent 2m pile in terms of Load Vs Settlement plot

It is concluded that Barrettes of same volume of concrete per meter can generate much higher capacity as the large diameter piles with a considerable saving in length there by bringing the settlements also to within serviceability limits. Settlements are also found to be within acceptable limits for the large size Barrettes as shown in Figure 13.

3.4 Barrettes of different orientation and Piles – horizontal capacities comparison

Barrettes horizontal capacities for an allowable 12mm horizontal deflection are estimated using the same design profile and same design method as that of piles. The capacities are estimated for single barrettes of 1.20 x 2.80m dimension and two sets of calculations are presented, with different load orientation. It can be seen from Figure 14 that when the widen dimension is oriented to the direction of loading, much higher horizontal load capacity is available as compared to the load oriented to the smaller dimension of 1.2m. Similar calculations are performed using L Pile, using same design profile and parameters and results are presented for 1.5m diameter piles, in Figure 15. It can be observed from the above three Figures that when barrette is oriented

towards the direction of loading for the design example, the horizontal capacity increases from 8MN to 14MN for the same allowable deflection of 12mm. Meanwhile, a large diameter pile of 1.5m diameter can generate only 3MN horizontal capacity for the same ground conditions. This demonstrates that the barrettes when oriented in the direction of high loading can resist the loads more efficiently and can bring in much better group efficiency.

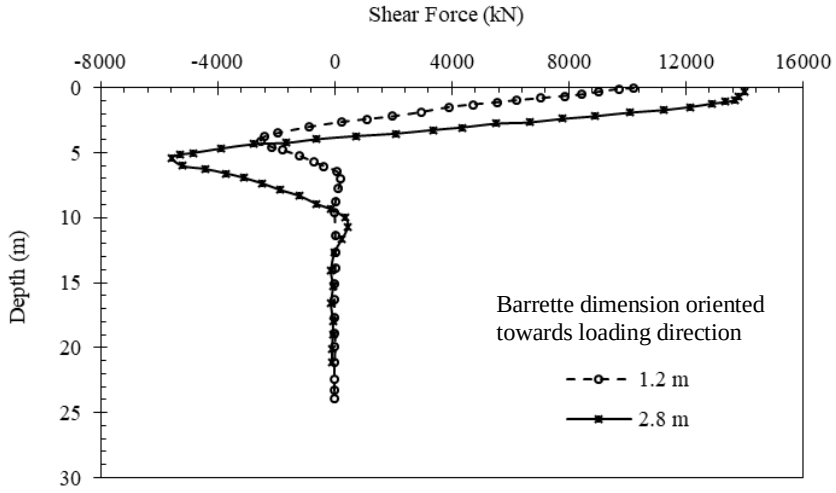

Fig. 14. Horizontal capacity of a single barrette of 1.2m x 2.8m dimension for 12mm deflection

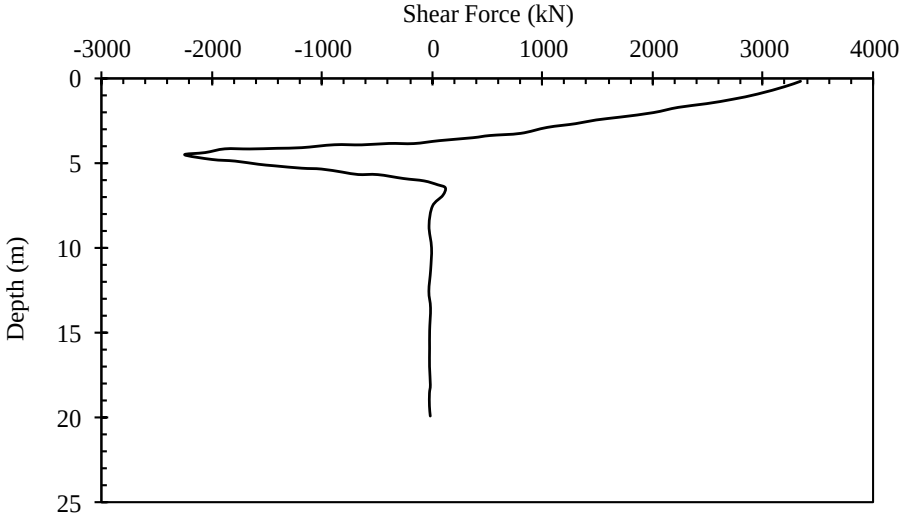

Fig. 15. Horizontal capacity of 1.5m diameter pile for 12mm deflection

Considering these facts presented above, and after careful design considerations, barrettes were selected as the efficient foundation system under the supertall building core in the example above. The grouping of piles and barrettes were then completed based on the overall structural layout, using 1.2m x 2.8m barrettes for the tower area thus efficiently transferring the critical load combinations including the earthquake loading.

4 Caisson Foundation

Due to the large cross sectional area with high rigidity, caisson foundations were generally believed to have high capacity against the axial as well as the lateral loading and subsequently immune to seismic loading. However, this assumption was found to impart a fallacious hope only after several bridges founded on caisson foundations were reported to encounter damage in Kobe 1995 earthquake. Thereafter, effect of seismicity, specifically lateral spreading induced by liquefaction on the stability of caisson foundation evoked interest among several researchers [23-25]. In this present study, the lateral stability of caissons under both static and dynamic conditions have been analyzed and finally an analytical approach for estimating the ultimate soil resistance has been proposed.

4.1 Under pseudo-static condition

For static loading condition, a case study was discussed, where peak ground acceleration values of different seismic motions were used to generate applied lateral loading.

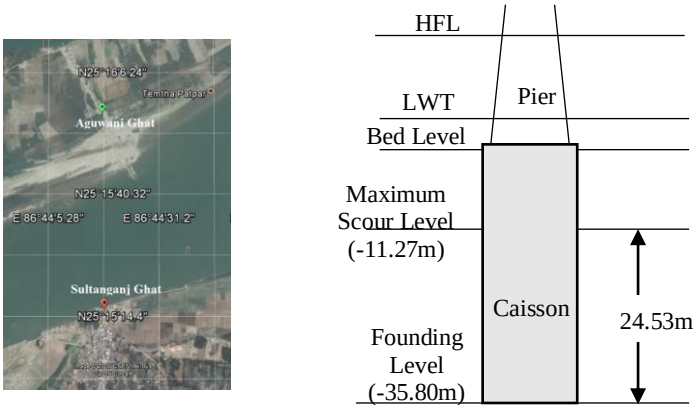

Fig. 16. (a) Location of the bridge across the river Ganga between Sultanganj and Aguwani Ghat, (b) schematic diagram of the caisson founded in soil

Bihar Rajya Pul Nirman Nigam Ltd. (BRPNNL, an undertaking of Govt. of Bihar) constructed a 2x2 Lane Bridge with footpath across the river Ganga between Sultanganj (Bhagalpur District) and Aguwani Ghat (Khagaria District) including navigational span of cable stayed and approaches (Connecting NH 31 and NH 80) in the State of Bihar (Fig. 16a). This bridge was proposed to be supported on circular shaped caisson foundations with a diameter of 14m. From the hydrological data, the Highest Flood level (HFL) and Lowest Water Table (LWT) have been found as 35.81m and 24.20m respectively. Although Lowest Bed Level has been measured as 18.630m but the Maximum scour Level has been calculated from available equations as (-) 11.27m. The well foundations were chosen to be founded at a level of (-) 35.80m. Therefore, the depth of the founding level of the caisson from the maximum scour level, as used for design purpose, was 24.53m, (Fig. 16b). Depending on the direct shear test results conducted on disturbed soil samples taken from the founding levels of caissons in the laboratory of BRPNNL at the strain rate of 1.25mm/min with porous plate on Top and Bottom of shear box, Intermediate shear failure mode has been decided to be chosen for SBC calculation. This decision was made due to the angle of internal friction (ϕ) values (30.5o) lying in the typical range of Intermediate shear failure mode i.e. between 28o and 36o. Following IS 6403-1981 [26] and IRC 78-2014 [27] and, the SBC for this particular project was calculated as 210.31 t/m2.

The horizontal seismic acceleration coefficient values i.e. PGAs multiplied with the applied vertical loading were used as horizontal loading following pseudo-static approach. In this analysis, earthquake input motions of Bhuj 2001, Sikkim 2011, Loma Prieta 1989 and El-Centro 1979 with PGA values of 0.106g, 0.201g, 0.279g and 0.43g respectively were used. A fraction of the estimated SBC, used as a multiplier for the seismic coefficient values, was applied at the caisson head to replicate the loads coming from superstructure. A 3D model in the finite element software PLAXIS3D [15] was used to simulate the lateral stability analysis.

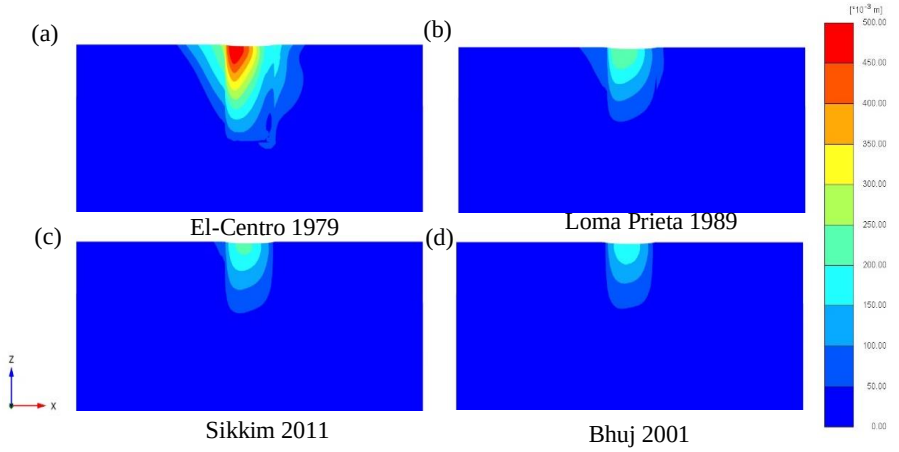

Fig. 17. Displacement contours under different pseudo-static loading - (a) El-Centro 1979, (b) Loma Prieta 1989, (c) Sikkim 2011, (d) Bhuj 2001

Mohr-Coulomb constitutive model was incorporated in the numerical analysis for capturing the caisson behavior. In terms of boundary condition, the vertical sides of the soil domain were restricted to horizontal movement, whereas fixity condition was adapted for the bottom side to make it restrain from all directions. The caisson was modelled using the approach of rigid body analysis. In rigid body, the relative displacement between two points within the body remain same for both before and after the application of loads, which demonstrates the fact that the caisson will undergo rotation and/or translation depending upon the type of loading, but will not bend with respect to its longitudinal axis. This behavior replicates the massive and heavy structures of caisson high stiffness contrast as compared to soil. Figure 17 illustrates the contour plots of displacements for different values of applied horizontal loading. The effect of the vertical load was found to be prominent for lower values of lateral loads.

The passive earth pressure diagrams generated due to the gradually increasing lateral loads have been shown in Figure 18. Although the lateral earth pressure was found to increase with the increment of the horizontal load following the conventional trend, the formation of the passive pressure distribution along the caisson height demonstrated an interesting phenomenon. The lateral loads demonstrated in this pseudo-static approach were not large enough to produce the ultimate soil resistance. For lower PGA values, the caisson experienced a full translation movement. However, with increment of loading, a coupling of rotation and translation was found to happen with an upliftment of the point of rotation along caisson height.

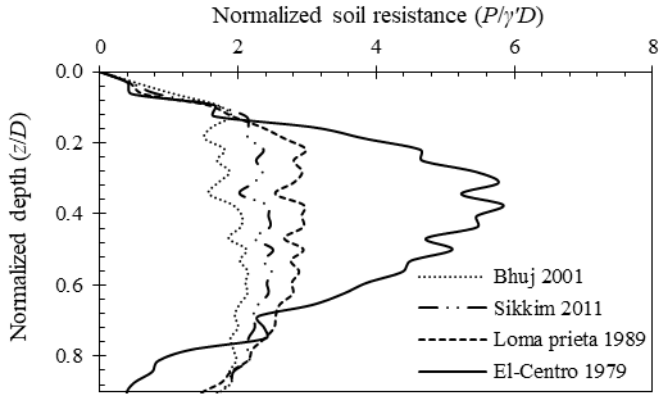

Fig. 18. Distribution of soil resistance along caisson height for different pseudo-static loading

4.2 Under dynamic loading condition

A complete 3D model was formed to capture the behavior of the caisson foundations under the effects of lateral spreading due to liquefaction. The extent of the model was set to around 40 times the width of the caisson with caisson placed at the center of the soil domain to eliminate the boundary effect on soil-structure interaction. The depth of soil layer was kept up to the base of caisson where input motion has been provided. Compliant base boundary condition has been employed at the bottom of the domain to

account for both absorption and application of dynamic input while the top surface was kept in free condition to simulate the flow following liquefaction. Ground water table has been considered at surface parallel to inclined ground. To facilitate free flow of soil during lateral spreading, the top ground surface has been kept in inclination with a certain percent of slope with the horizontal line throughout the domain. In this dynamic analysis, UBC3D-PLM, a specific constitutive model capable of capturing the rapid generation of excess pore pressure and subsequently degradation of soil strength during liquefaction, was used. This constitutive model is a generalized 3-D upgradation of UBCSAND i.e. University of British Columbia Sand model and has been demonstrated by Makra [28].

Table 6. Soil properties used in centrifuge study performed by Olson et al. (2017)

Parameter	Values
Relative density (D_r)	33 %
Constant volume friction angle, ϕ'_{cv}	33°
Peak effective stress friction angle, ϕ'	37°
SPT N value	~6 to 8

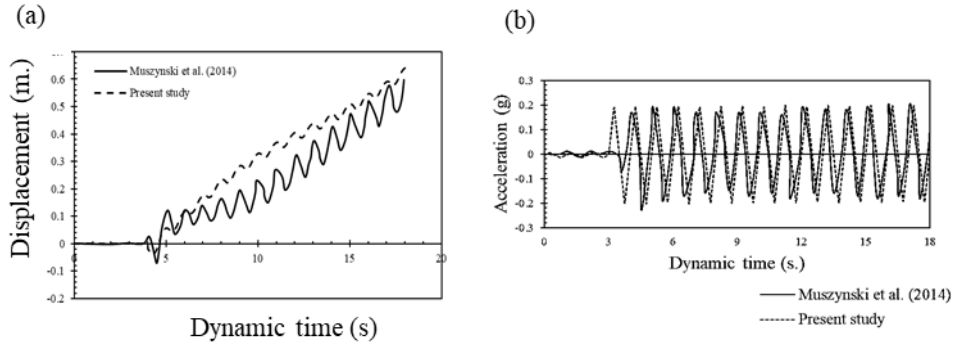

Fig. 19. (a) Comparison of displacement at 5 m depth (free-field), (b) comparison of base acceleration with input motion

In the analysis, 10 % damping has been considered which is consistent with the practical range for soils. The mesh sensitivity analysis was performed following checking for the required element size from the time step calculation and seismic wave propagation criteria. The illustrated numerical model was compared with the results obtained from the experimental study performed by Muszynski et al. [29] and Olson et al. [30] in centrifuge at 50-g condition as a part of a NEES study at RPI. The soil properties used in the experimental setup has been demonstrated in Table 6. For validation purpose, the bottom 2m layer of the soil domain was modelled as non-liquefiable layer, where the remaining part was modelled as per the liquefiable soil

properties shown in [30]. The comparison between the centrifuge study and numerical analysis has been shown in Figure 19. Both the base acceleration and horizontal displacement at a depth of 5 m from the ground surface estimated by FE model were found to be in good agreement with the experimental results.

4.3 Proposed analytical model

Experimental results and above mentioned FE analysis depicted about the formation of passive wedges due to increment of lateral loading. As per strain wedge model [31] and wedge failure analysis [32, 33], 3D passive wedge with planar rupture surface can be conceptualized from the stressed zones developed in front of the embedded foundation. The final dimensions of the 3D wedge formation to be considered for calculation depends upon the finally developed stressed zone as measured from the experiments (see Figure 20). The two angles as shown in the figure i.e. α and β along with the height of the passive wedge (h) constitute a vital geometrical relationship for the three-dimensional passive wedge development.

In the present study, both pseudo-static and modified pseudo-dynamic approaches have been discussed using method of limit equilibrium. The forces acting on the 3D passive wedge include reactions forces coming from soil and caisson and tangential forces to capture the vertical side reaction. In pseudo-static approach, horizontal and vertical seismic acceleration coefficients i.e. k_h and k_v have been considered to incorporate seismicity in the analysis. Following the horizontal and vertical force equilibrium in pseudo-static approach [34, 35], seismic passive earth pressure coefficient can be formulated as below:

$$K_{dpe} = \frac{2P_{dpe}}{\gamma h^2} = \frac{\left(\frac{1}{\tan\alpha}\right)\left\{\left(\frac{2\lambda h\tan\phi}{3D\tan(\alpha+\phi)}\right)-\left(1+\frac{2h\tan\phi}{3D\tan\alpha}\right)\left\{(1-k_v)-k_h\cot(\alpha+\phi)\right\}\right\}}{\left\{\sin\delta-\cos\delta\cdot\cot(\alpha+\phi)\right\}} \quad (2)$$

Seismic passive earth pressure distribution along with caisson height has also been calculated by differentiating the earth pressure values:

$$p_{dpe} = \frac{dP_{dpe}}{dz} = \frac{\left(\frac{\gamma z}{\tan\alpha}\right)\left\{\left(\frac{\lambda z\tan\phi}{D\tan(\alpha+\phi)}\right)-\left(1+\frac{z\tan\phi}{D\tan\alpha}\right)\left\{(1-k_v)-k_h\cot(\alpha+\phi)\right\}\right\}}{\left\{\sin\delta-\cos\delta\cdot\cot(\alpha+\phi)\right\}} \quad (3)$$

In modified pseudo-dynamic approach [36-38], seismic inertia forces have been considered to act on the passive wedge. For analyzing the ultimate soil resistance using this approach, 4 assumptions were taken into account as shown below:

- Wave was considered to be propagating vertically in a Kelvin-Voigt homogeneous medium
- A constant value of shear modulus was assumed throughout the soil
- Base displacements were assumed to obtain the solutions

• Following boundary conditions were imposed upon; (a) at ground surface i.e. z = 0, shear stress is zero and (b) the displacements at z = H i.e. at the base coincide with the base displacements

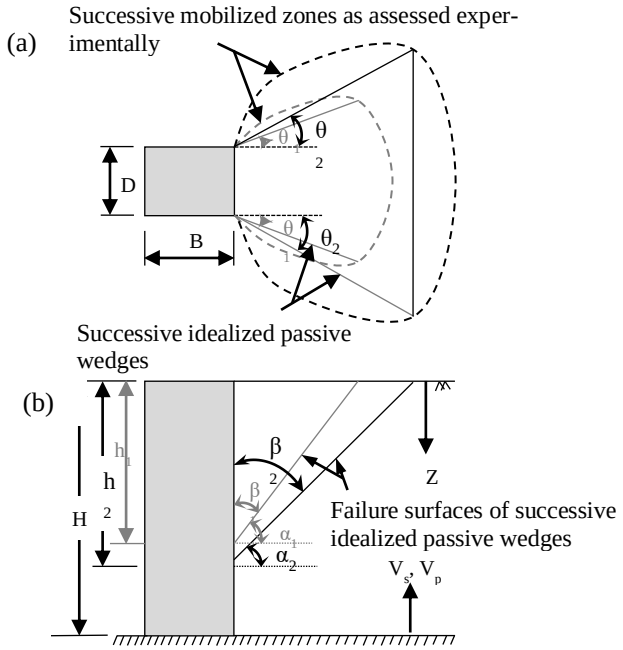

Fig. 20. (a) Plan view of the idealized passive wedge developed from mobilized stressed zones, (b) sectional view of the developed idealized passive wedge

Consideration of damping in soil by assuming Kelvin-Voigt model [39] and amplification of wave during its propagation through soil in modified pseudo-dynamic method eventually overcome the limitations involved in the both pseudo-static and pseudo-dynamic approach [40, 41]. For lower values of normalized frequency, damping has been found to play a major role in amplifying the acceleration from base to surface, however the impact is seen to decrease with higher frequency values. Seismic inertia forces used in the force equilibrium in modified pseudo-dynamic approach have been demonstrated as follows where the horizontal and vertical seismic accelerations (ah and av) were obtained by differentiating the base displacements [36-38],

$$Q_h(\alpha,t) = \int_{z=0}^{z=h} m(z)_{wedge}\, a_h(z,t) \qquad (4) \quad \text{And} \quad Q_v(\alpha,t) = \int_{z=0}^{z=h} m(z)_{wedge}\, a_v(z,t) \qquad (5)$$

Where, $m\,(z)_{\text{wedge}}$ can be written as the mass of a thin element with thickness *dz* of the idealized passive wedge

$$m(z)_{wedge} = \frac{\gamma_{dry}(h-z)}{g\tan\alpha}\left(D + \frac{(h-z)\tan\theta}{\tan\alpha}\right)dz \quad (6)$$

After following the same methodology as adapted in pseudo-static approach, earth pressure distribution have also been estimated. By considering the unit weight of soil as saturated or submerged instead of dry, the analysis procedures discussed above were extended for submerged soil also [42]. In this approach, both hydrostatic and hydrodynamic pressure were added with the lateral soil resistance to obtained total passive pressure. For validation purpose, the earth pressure coefficient values calculated using 3D idealized passive wedge have been compared with the three-dimensional earth pressure theories used for limit analysis in static condition [43, 44].

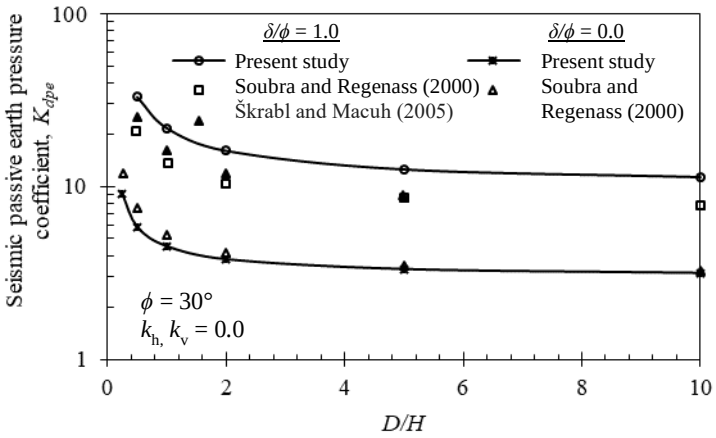

Fig. 21. Comparison of the three-dimensional static passive earth pressure coefficients

Figure 21 shows a good agreement between the coefficient values for lower values of soil-caisson interface friction angle. However, for higher values, present analysis overestimated the limit analysis results due to the assumption of planar failure surface. Typical variation of seismic passive earth pressure coefficient values in dry condition for different embedment ratios, soil friction angle values have been shown in Figure 22 (a-d). The decreasing coefficient values with increasing *D*/*H* values enhance the applicability of 3D wedge failure analysis as compared to the conventionally used plain strain assumption. For a very high caisson width, the passive earth pressure values acting on a rigid caisson in both static and seismic loading conditions match exactly with the Coulomb earth pressure values. This shows the acceptability of the proposed methodology in plain strain condition also.

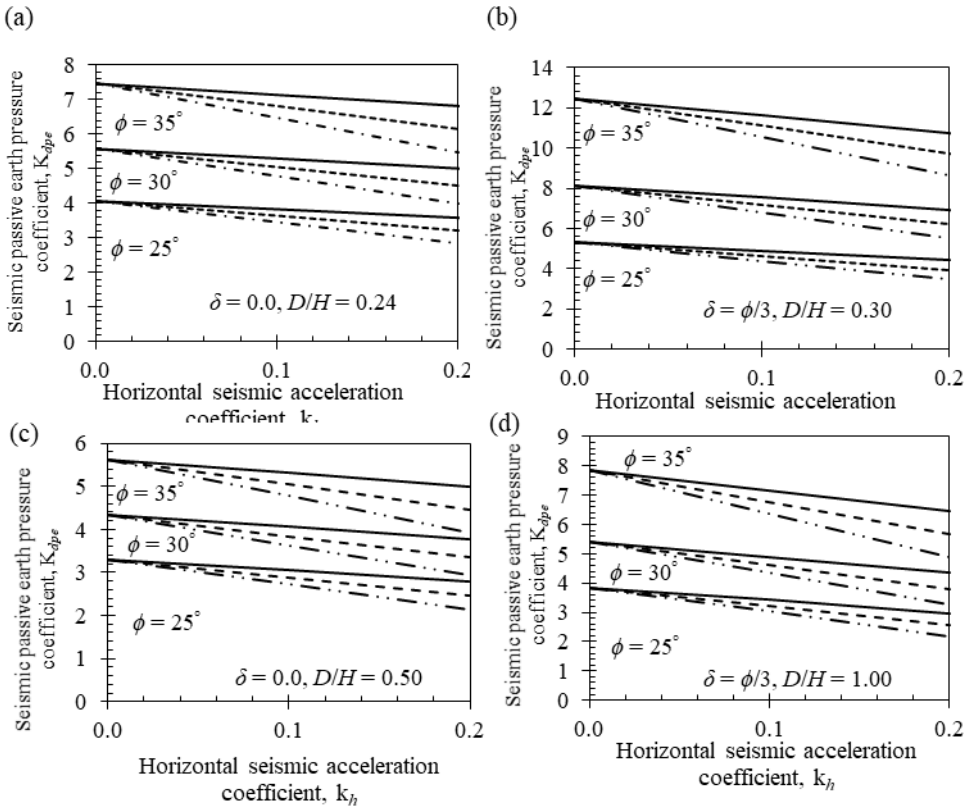

Fig. 22. 3D seismic passive earth pressure coefficient values for different soil-caisson interface friction values (δ) and embedment ratios (D/H) – (a) δ = 0.0, D/H = 0.24, (b) δ = ϕ/3, D/H = 0.30, (c) δ = 0.0, D/H = 0.50, (d) δ = ϕ/3, D/H = 1.00

5 Conclusions

Behavior of different types of deep foundations that are used to provide stability in bridges and high-rise buildings under both static and seismic loading conditions are discussed in this paper. Case histories of three different foundations systems, namely, long pile foundations, barrette foundations and rigid caisson foundations with soil-structure interaction analysis have been discussed in detail. The analysis of Mumbai Trans Harbour Link founded on large diameter piles has been carried out by considering soil-structure interaction of bridge foundation using finite element-based computer program, PLAXIS3D. The displacement and relative shear stress along the soil-pile interface surface due to combined loading along with the structural forces in piles, axial force, bending moment and shear force under combined static and earthquake loadings have been presented in this paper. From the numerical analysis results, the existing foundation system was found to be able to sustain the earthquake loading.

Later, a case study of a 380m tall tower was discussed where based on a comparative study of performances, barrette foundation was selected to cater the heavy loads as an alternative to the pile foundation. The loading direction and orientation of barrettes along with the higher frictional resistance were found to affect both the horizontal and vertical capacity as compared to cast-in-situ large diameter piles. The efficacy of barrettes over piles in terms of cost effectiveness has been recognized, however the suitability of barrettes under earthquake conditions is yet to be proven. Lastly, a case study of a bridge founded on rigid caisson foundation was studied following pseudo-static approach where PGA values of different earthquake motions were used as a fraction of total lateral load. The passive wedge developed in front of the rigid caissons for both pseudo-static and dynamic condition has been considered in this study to initiate an analytical approach where a limit equilibrium method of all the relevant forces acting on the 3D passive wedge was taken into account. Both pseudo-static and modified pseudo-dynamic approaches have been discussed in this paper by considering soil as Kelvin-Voigt model with stress free surface condition. The string of dynamic soil-structure analyses demonstrated in this study forms a bridge between case histories and theoretical analysis by addressing the necessity of an efficient, cost-effective solution for foundation systems under earthquake conditions.

Acknowledgements

The authors want to acknowledge the funding received from L&T Construction Infrastructure IC, India and Bihar Rajya Pul Nirman Nigam Ltd. (BRPNNL), Govt. of Bihar, India to carry out some of these industrial projects with soil investigation reports and other necessary input data.

References

1. Poulos, H.G., Badelow, F.: Geotechnical parameter assessment for tall building foundation design. International J of High-Rise Buildings 4(4), 227–239 (2015).
2. Poulos, H.G.: Tall Building Foundation Design. CRC Press, Taylor & Francis Group, USA (2017).
3. Katzenbach, R., Leppla, S., Choudhury, D.: Foundation Systems for High-Rise Structures. CRC Press, Taylor & Francis Group, USA (2016).
4. Phanikanth, V.S., Choudhury, D., Reddy, G.R.: Behavior of single pile in liquefied deposits during earthquakes. International Journal of Geomechanics 13(4), 454-462 (2013).
5. Zhang, Y., Salgado, S., Dai, G., Gong, W.: Load tests on full scale bored pile groups. In: Proceedings of the 18th International Conference on Soil Mechanics and Geotechnical Engineering, Paper No. 2119 (2013).
6. Manoj, S., Choudhury, D., Alzaylaie, M.: Value engineering using load-cell test data of barrette foundations - La Maison, Dubai. Proceedings of the Institution of Civil Engineers - Geotechnical Engineering, ICE. doi: 10.1680/jgeen.19.00246 (2020).
7. Zhang, L.M.: Behavior of laterally loaded large-section barrettes. J Geotech and Geoenviron Eng 129(7), 639-648 (2003).

8. IRC 45: Recommendations for Estimating The Resistance of Soil Below The Maximum Scour Level in The Design Of Well Foundations Of Bridges. Indian Road Congress, New Delhi (1972).
9. Biswas, S., Choudhury, D.: Behavior of caisson foundations under lateral loading in layered cohesive soil. In: Geo-Congress 2020: Foundations, Soil Improvement, and Erosion, Geotechnical Special Publication No. GSP 315:23-32, ASCE, USA (2020).
10. IS 1893-Part 1: Criteria for earthquake resistant design of structures- Part 1- General provisions and buildings. Bureau of Indian Standards, New Delhi, India (2016).
11. Duncan, J.M., Buchignani, A.L.: An engineering manual for settlement studies. Department of Civil Engineering, University of California, Berkeley (1976).
12. Darendeli, M.B.: Development of a new family of normalized modulus reduction and material damping curves. PhD dissertation, University of Texas at Austin, Austin, Texas (2001).
13. Seed, H.B., Wong, R.T., Idriss, I.M., Tokimatsu, K.: Moduli and damping factors for dynamic analyses of cohesionless soils. Journal of Geotechnical Engineering, ASCE. 112(11):1016-1032 (1986).
14. EPRI: Guidelines for determining design basis ground motions, early site permit demonstration program. Vol. 1, RP3302, Electric Power Research Institute, Palo Alto, California (1993).
15. PLAXIS 3D v2017.01 Suite: [Computer software]. PLAXIS BV, Netherlands (2017).
16. PLAXIS3D: Material models manual. Plaxis B. V. Netherlands, 45-52 (2017).
17. Hoek, E., Brown, E.T.: The Hoek-Brewn failure criterion. In: the Proc. 15th Canadian Rock Mechanics Symp. 31-38 (1988).
18. Hudson, M:, Idriss, I.M., Beikae, M.: User's manual for QUAD4M. Center for Geotechnical Modeling, University of California, Davis (1994).
19. Patil, M., Choudhury, D., Ranjith, P.G., Zhao, J.: Behavior of shallow tunnel in soft soil under seismic conditions. Tunnelling and Underground Space Technology 82:30-38 (2018).
20. Poulos, H.G.: Tall buildings and deep foundations–Middle East challenges. In: Proc. 17th Int. Conf. Soil Mech. Geotechnical Engineering, Amsterdam. 4:3173-3205 (2009).
21. Charif, K.H., Najjar, S.S.: Side friction along drilled shafts in weak carbonate rocks. The Art of Foundation Engineering Practice – guide 190 – 204 (2010).
22. Russo, G., Abagnara, V., Poulos, H.G., Small, J.C.: Re-assessment of foundation settlements for the Burj Khalifa, Dubai. Acta Geotechnica, 8(1), 3-15 (2013).
23. Gerolymos, N., Gazetas, G.: Winkler model for lateral response of rigid caisson foundations in linear soil. Soil Dynamics and Earthquake Engineering 26(5), 347-361 (2006a).
24. Gerolymos, N., Gazetas, G.: Development of Winkler model for static and dynamic response of caisson foundations with soil and interface nonlinearities. Soil Dynamics and Earthquake Engineering 26(5), 363-376 (2006b).
25. Mondal, G., Prashant, A., Jain, S. K.: Simplified seismic analysis of soil–well–pier system for bridges. Soil Dynamics and Earthquake Engineering 32(1), 42-55 (2012).
26. IS 6403: Indian Standard Code of Practice for Determination of Breaking Capacity of Shallow Foundations, Bureau of Indian Standards, New Delhi (1981).
27. IRC 78: Standard Specifications and code of Practice for Road Bridges, Section: VII, Foundation and Structure, Indian Road Congress, New Delhi (2014).
28. Makra, A.: Evaluation of the UBC3D-PLM constitutive model for prediction of earthquake induced liquefaction on embankment dams. (M.Sc thesis, TU Delft) (2013).

29. Muszynski, M.R., Olson, S.M., Hashash, Y.M., Phillips, C.: Repeatability of centrifuge tests containing a large, rigid foundation subjected to lateral spreading. Geotechnical Testing Journal 37(6), 1002-1015 (2014).
30. Olson, S.M., Hashash, Y.M., Muszynski, M.R., Phillips, C.: Passive wedge formation and limiting lateral pressures on large foundations during lateral spreading. J. Geotech. Geoenviron. Eng. 143(7):04017027 (2017).
31. Ashour, M., Norris, G., Pilling, P.: Lateral loading of a pile in layered soil using the strain wedge model. Journal of Geotechnical and Geoenvironmental. Eng. 124(4), 303–315 (1998).
32. Bowman, E.R.: Investigation of the lateral resistance to movement of a plate in cohesionless soil. Doctoral dissertation, University of Texas at Austin, Austin, Texas, (1958).
33. Kim, Y., Jeong, S., Lee, S.: Wedge failure analysis of soil resistance on laterally loaded piles in clay. J. Geotech. Geoenviron. Eng. 137(7), 678-694 (2010).
34. Lancellotta, R. Lower-bound approach for seismic passive earth resistance. Géotechnique 57(3), 319-321 (2007).
35. Biswas, S., Choudhury, D.: Seismic soil resistance for caisson design in sand. Proceedings of the Institution of Civil Engineers-Geotechnical Engineering 172(1), 67-75 (2019).
36. Bellezza, I., D'Alberto, D., Fentini, R.: Pseudo-dynamic approach for active thrust of submerged soils. Proceedings of the Institution of Civil Engineers-Geotechnical Engineering 165(5), 321-333 (2012).
37. Bellezza, I.: Seismic active earth pressure on walls using a new pseudo-dynamic approach. Geotechnical and Geological Engineering 33(4), 795-812 (2015).
38. Rajesh, B.G., Choudhury, D.: Generalized seismic active thrust on a retaining wall with submerged backfill using a modified pseudodynamic method. International Journal of Geomechanics 17(3), 06016023_1-10 (2017).
39. Kramer, S.L.: Geotechnical earthquake engineering, Prentice-Hall. New Jersey (1996).
40. Steedman, R.S., Zeng, X.: The influence of phase on the calculation of pseudo-static earth pressure on a retaining wall. Géotechnique. 40(1), 103-112 (1990).
41. Choudhury, D., Nimbalkar, S.: Seismic passive resistance by pseudo-dynamic method. Géotechnique 55(9), 699-702 (2005).
42. Ebeling, R.M., Morrison, E.E.: The seismic design of waterfront retaining structures. Technical Rep. No. ITL-92-11, U.S. Army Corp of Engineers, Washington, DC (1992).
43. Škrabl, S., Macuh, B.: Upper-bound solutions of three-dimensional passive earth pressures. Canadian Geotechnical Journal 42(5), 1449-1460 (2005).
44. Soubra, A. H., Regenass, P.: Three-dimensional passive earth pressures by kinematical approach. Journal of Geotechnical and Geoenvironmental Engineering 126(11), 969-978 (2000).